

# Silicalite-1 Supported ZnO as an Efficient Catalyst for Direct **Propane Dehydrogenation**

Jie Liu, [a, b] Yong Liu, \*[a] Hongchao Liu, [a] Yi Fu, [a, b] Zhiyang Chen, [a] and Wenliang Zhu\*[a]

Direct propane dehydrogenation (PDH) is an attractive onpurpose strategy for propylene production. Compared with high-priced Platinum and toxic Chromium oxide, ZnO based catalysts attract wide attention due to its low-cost and environment-friendly character. Herein we report silicalite-1 supported ZnO catalysts for PDH reaction. They exhibited an excellent catalytic performance. The catalyst with 5 wt% Zn exhibited the best propane yield with propane conversion reaching 49% and

propylene selectivity around 90% at a space velocity of 5000 ml·g<sup>-1</sup>·h<sup>-1</sup>. Characterization with  $N_2$  adsorption, XRD, SEM, TEM, EDS, NH<sub>3</sub>-TPD, UV-vis, XPS, <sup>29</sup>Si MAS NMR, FT-IR, Py-IR and TGA reveal that the high activity and stability can be attributed to the dispersed ZnO species due to the interaction between silanol nests of silicalite-1 support and ZnO species. This study may open a promising way for development of highly efficient PDH catalysts.

frequently dispersed and stabilized on supports. Schweitzer

#### Introduction

Propylene is a vital and basic building block and used for production of a variety of chemicals such as polypropylene, acrylic acid and acrylonitrile.[1-5] Propylene is generally produced from petroleum-derived steam cracking and fluid catalytic cracking (FCC) process. However, the current production capacity cannot fully meet the rapidly increasing demand. [4,5] As the hydraulic fracturing technology improves, large volumes of shale gas containing propane can be extracted and direct propane dehydrogenation (PDH) attracts wide attention for propylene production with the advantage of less byproducts.[3] Pt and CrO<sub>x</sub> based catalysts are widely used in industrial PDH process and the representative processes are Catofin and Oleflex, which were developed by UOP and Lummus, respectively.[1,3,6-10] However, the high cost of Pt, strong toxicity of CrO<sub>x</sub> in addition to the fast deactivation still hinder their wide applications. Therefore, it is desirable to develop alternative catalysts with low-cost and environment-benign nonnoble catalysts.

Among Zn, V, Zr, Co and Fe-based catalysts, [11-15] Zn-based catalysts have received more attention due to its low-cost and environment-friendly properties. Both isolated Zn<sup>2+</sup> species and nanosized ZnO assemblies were active for PDH reactions. [16] However, small ZnO assemblies were generally unstable especially under harsh reaction conditions<sup>[17]</sup> and they were

et al. reported an over 95% propylene selectivity although the catalytic activity was low over the isolated Zn2+ supported on silica exhibiting Lewis acid property. [18] A TiZrO<sub>x</sub>-supported ZnOcontaining catalyst was reported to exhibit excellent PDH catalytic performance and isolated tricoordinated Zn<sup>2+</sup> species were concluded as the active sites. Its intrinsic activity was enhanced when ZrO<sub>2</sub> was promoted by TiO<sub>2</sub>. [19] ZnO/Al<sub>2</sub>O<sub>3</sub> modified by a trace amount of Pt showed excellent PDH activity, in which Lewis acidic ZnO served as active sites and Pt worked as a promoter by increasing the Lewis acidity of Zn<sup>2+</sup>.<sup>[20]</sup> Furthermore, it was much more stable than the unpromoted ZnO/Al<sub>2</sub>O<sub>3</sub> catalyst. In addition, zeolites were also employed for dispersion of ZnO clusters. For instance, well dispersed small ZnO nanoclusters anchored in the framework of dealuminated Beta zeolite was shown with a high activity and propylene selectivity. [17] Chen et al. reported that a high PDH activity was obtained over high silica H-ZSM-5 supported ZnO catalyst. The propylene selectivity and reaction stability increase with elevating SiO<sub>2</sub>/Al<sub>2</sub>O<sub>3</sub> ratios while the strong acidity of low-silica H-ZSM-5 favors the side reactions and ZnO aggregation. [21] In comparison, silicalite-1 (S-1) zeolite has the same MFI topology without strong acidity. Recently, Li et al. contructed Zncontaining catalysts Zn@S-1 through in-situ hydrothermal synthesis for PDH reaction and the partially reduced zinc cations were identified as the active sites.<sup>[22]</sup> Furthermore, the presence of abundant defects makes S-1 widely used as catalyst support.[23] We wonder whether S-1 is an effective support to directly disperse and stabilize active ZnO species for PDH

Therefore, S-1 supported ZnO catalysts were prepared by a simple impregnation method and used for PDH reaction, which demonstrated excellent PDH performance. The effect of Zn loading on the catalytic performance was investigated. For comparision, ZnO supported on SiO<sub>2</sub>, Al<sub>2</sub>O<sub>3</sub> and high-silica H-ZSM-5 were also synthesized for PDH reaction. The results show that 5%Zn/S-1 exhibited a much higher propylene yield than  $5\%Zn/SiO_2$ ,  $5\%Zn/Al_2O_3$  and 5%Zn/H-ZSM-5 (SiO<sub>2</sub>/Al<sub>2</sub>O<sub>3</sub> = 360)

[a] J. Liu, Prof. Y. Liu, Prof. H. Liu, Y. Fu, Dr. Z. Chen, Prof. W. Zhu National Engineering Laboratory for Methanol to Olefins Dalian National Laboratory for Clean Energy Dalian Institute of Chemical Physics Chinese Academy of Sciences Dalian 116023 (P. R. China) E-mail: vonal@dicp.ac.cn wlzhu@dicp.ac.cn

[b] J. Liu, Y. Fu

University of Chinese Academy of Sciences Beiiina 100049 (P. R. China)

Supporting information for this article is available on the WWW under https://doi.org/10.1002/cctc.202101069



under the same reaction condition. The role of ZnO species and support in Zn/S-1 catalysts was elucidated on the basis of detailed characterizations and PDH catalytic performance.

#### **Results and Discussion**

#### Catalytic activity, selectivity, and stability

Figure 1 shows that there is almost no conversion of C<sub>3</sub>H<sub>8</sub> on S-1 zeolite. In comparison, the C<sub>3</sub>H<sub>8</sub> conversion increases obviously with introduction of Zn species. The initial propane conversion jumps up from 5.7% to 40.7% as Zn loading increases from 1% to 3%. It further increases to 49.3% with Zn loading increasing to 5%. These results suggest that the catalytic activity is attributed to the presence of Zn species. It is worth noting that all Zn/S-1 catalysts with Zn loading varying in the range of 1-5% exhibit a good stability. For instance, propane conversion only slightly decreases from 40.7% to 36.5% for 3%Zn/S-1 after 6 h reaction. In comparison, the 10%

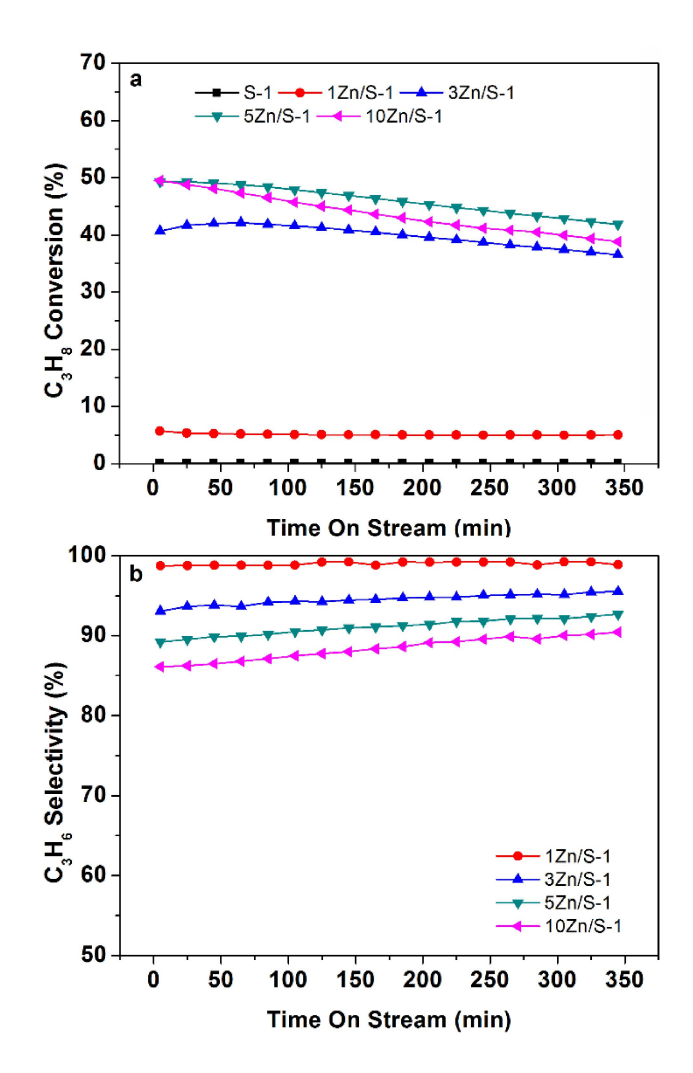


Figure 1. Catalytic performance of different catalysts in PDH reaction. (a) Propane conversion; (b) Selectivity to propylene. Reaction conditions: T=550 °C, P=0.1 MPa, GHSV=5000 mLh<sup>-1</sup>  $g_{cat}^{-1}$ , C<sub>3</sub>H<sub>8</sub>/Ar=5/95.

Zn/S-1 exhibits similar initial propane conversion with 5%Zn/ S-1 but it suffers a slightly faster deactivation probably due to the formation of a small number of larger ZnO particles with the increase of Zn loading, as evidenced by XRD (Figure 4) and TEM (Figure S3) results. A high initial propylene selectivity ranging from 89.2% to 98.8% is achieved on Zn/S-1 catalysts with Zn loading from 1% to 5% with a small amount of methane, ethane, ethylene and C<sub>4+</sub> species (Figure 1b and Table S1).

The propylene yields are summarized in Table S1, which shows that 5%Zn/S-1 gives a highest yield (44.0%) among the studied catalysts. As show in Figure 2, the propane conversions on  $5\%Zn/SiO_2$  and  $5\%Zn/Al_2O_3$  are only 0.32% and 1.67%, respectively. Although 5%Zn/H-ZSM-5 gives a higher initial propane conversion (66.2%) than 5%Zn/S-1, its initial propylene selectivity is only 39.8% thus exhibiting a low propylene yield of only 26.3%. This could be attributed to the strong Brønsted acid sites on H-ZSM-5 zeolite, which catalyze undesirable side reactions.  $^{[24]}$  Although the propylene selectivity on  $5\,\%\text{Zn/H-}$ ZSM-5 increases with time on stream, it remains as low as only 60.7% after 6 h time on stream.

Considering the thermodynamic constraints, PDH reactions were also carried out over 5%Zn/S-1 catalyst at different reaction temperatures of 500, 525, 550 and 575 °C. As shown in Figure 3, the initial propane conversion significantly increases from 18.8% to 66.7% while propylene selectivity decreases with the stepwise increasing temperature. The propylene selectivity at 575 °C decreases significantly due to the facilitated side reactions at high temperature. [25] Therefore, the most suitable temperature is chosen as 550°C in order to achieve high propane conversion and propylene selectivity simultaneously. Figure S1 shows that a higher space velocity benefits selective formation of propylene. For example, propane conversion only decreases slightly, while propylene selectivity improves with the GHSV increasing from 4000 to 8000 mLg<sup>-1</sup> h<sup>-1</sup>. In terms of propylene space-time-yield (STY), 5 %Zn/S-1 exhibits a comparable value compared with zeolite supported Zn-based catalysts

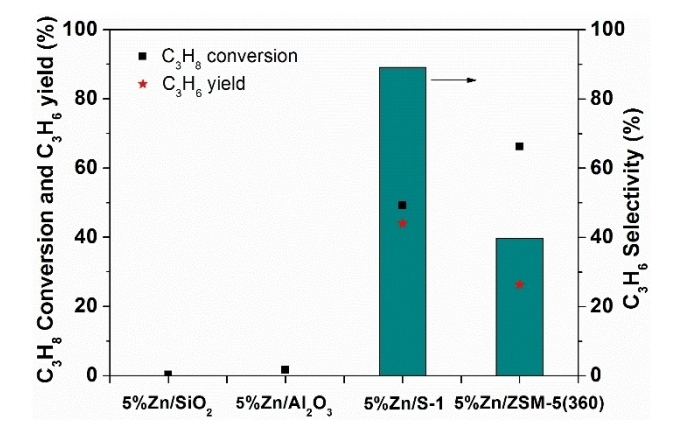
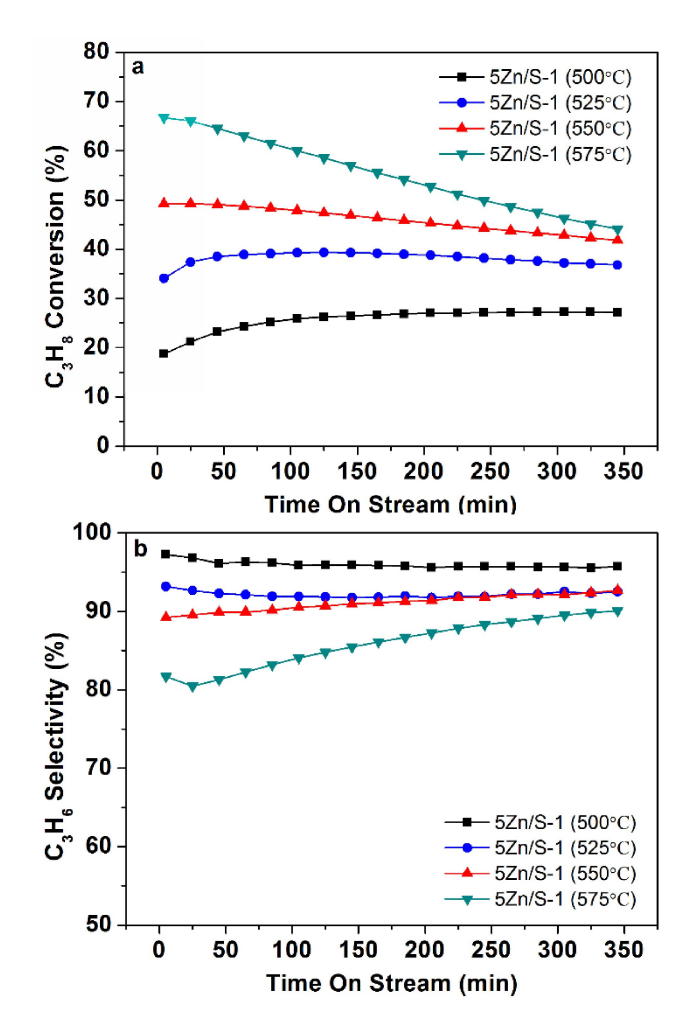


Figure 2. Initial catalytic performance of the supported ZnO-based catalysts in PDH reaction, Reaction conditions: T=550 °C, P=0.1 MPa. GHSV = 5000 mL h<sup>-1</sup>  $g_{cat}^{-1}$ ,  $C_3H_8/Ar = 5/95$ .





**Figure 3.** Catalytic performance of 5%Zn/S-1 catalyst in PDH reaction at different reaction temperature. (a) Propane conversion; (b) Selectivity to propylene. Reaction conditions: P = 0.1 MPa, GHSV = 5000 mL  $h^{-1}g_{cat}^{-1}$ ,  $C_3H_8$ /Ar = 5/95.

reported before under comparable reaction conditions (Table S2).

## Characterizations of the catalysts

The XRD patterns in Figure 4 show that the S-1 zeolite exhibits a typical MFI structure. Its crystal structure remains unchanged after being supported with ZnO. No diffraction peaks corresponding to ZnO are observed for the catalysts with Zn loading up to 5%, suggesting that Zn species are well dispersed or existing as tiny ZnO particles which are beyond XRD detection limitation. However, at 10% loading, weak diffraction peaks attributed to ZnO appear, indicating the growth of Zn species.

The SEM images in Figure S2 show that S-1 zeolite is well crystallized with a uniform size distribution about 100 nm. The introduction of Zn species has little influence on the morphology. The TEM images in Figure 5a and 5b show that small nanoparticles with an average particle size of 3.1 nm are distributed uniformly on the fresh 5%Zn/S-1 catalyst. The

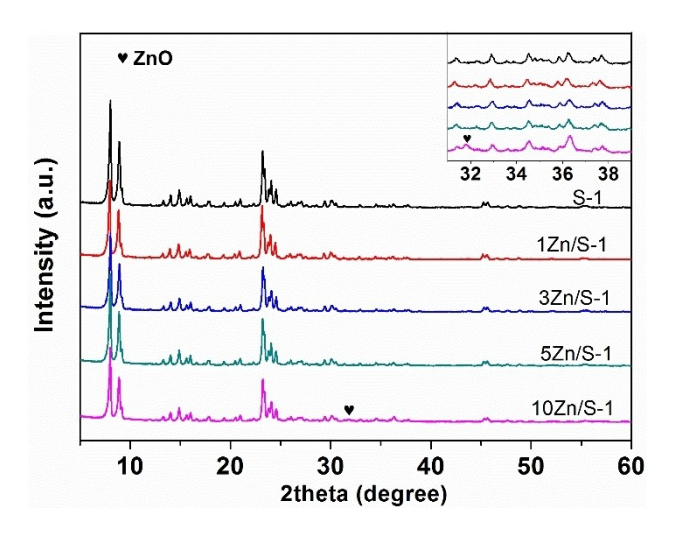
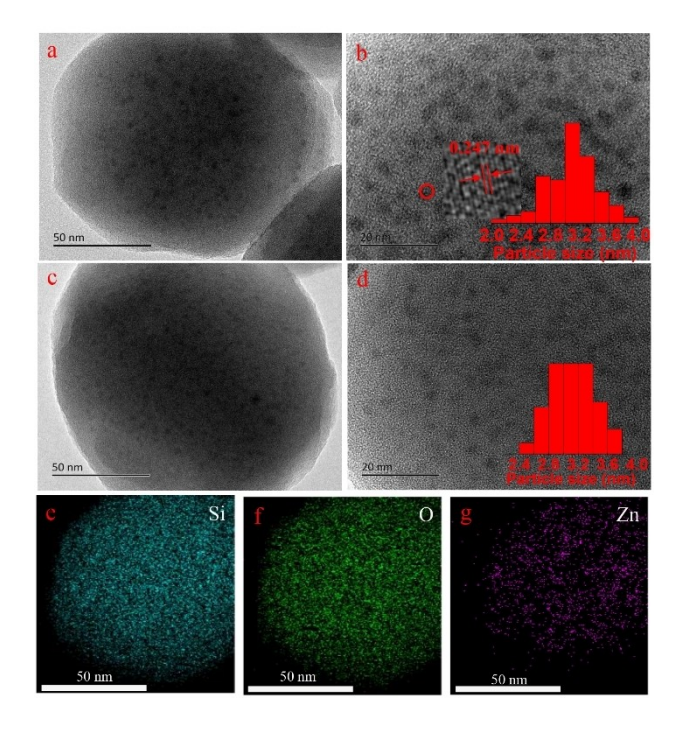


Figure 4. XRD patterns of S-1 zeolite and Zn/S-1 catalysts



**Figure 5.** TEM images of fresh 5%Zn/S-1 catalyst (a, b) and spent 5%Zn/S-1 (c, d); EDS mapping of fresh 5%Zn/S-1 catalyst (e, f, g).

HRTEM image inserted in Figure 5b shows an interplanar spacing 0.247 nm, which corresponds to the (101) plane of ZnO crystalline. Furthermore, the EDS mapping confirms the homogeneous distribution of Zn species (Figure 5). Large ZnO particles appear when the Zn loading increases to 10% (Figure S3), which is consistent with XRD. As shown in Figure 5c and 5d, the average particle size of the ZnO nanoparticles over the used 5%Zn/S-1 catalyst remains 3.1 nm and no obvious aggregation is observed in comparison with the fresh catalyst. The results demonstrate a good stability of the ZnO species on 5%Zn/S-1 catalyst.



N<sub>2</sub> physisorption results (Table 1) indicate that the specific surface area and pore volume gradually decrease with the increasing Zn loadings. Below 5% Zn loading, mainly the external surface area decreases, indicating that ZnO species are dispersed on the external surface. Meanwhile, it is reasonable to assume that some ZnO species deposit inside the zeolitic pores considering the slight decrease of microporous surface area.[27] As the Zn loading further increases to 10%, both the external surface area and the microporous surface area decrease. This may be attributed to large ZnO particles at a high Zn loading blocking the pore openings of S-1. [28]

The DR UV-vis in Figure 6 shows a band at around 370 nm and a weak shoulder one at about 265 nm upon introduction of zinc species to S-1 zeolite. These two bands are generally attributed to ZnO crystals on the external zeolite surface and subnanometric ZnO clusters inside zeolitic pores, respectively. [29] Furthermore, the intensity of the 370 nm band is enhanced with the increasing Zn loading, especially for Zn/S-1 catalyst with higher Zn loading such as 10 %Zn/S-1 indicating enhanced formation of ZnO species on the external surface.

NH<sub>3</sub>-TPD and Py-IR are employed to characterize the acidic properties of the catalysts considering that Zn species exhibiting Lewis acidity are generally considered as active sites in PDH reaction. [20] As shown in Figure 7a and Table 1, S-1 zeolite only

<b>Table 1.</b> Textural properties of S-1 and Zn/S-1 catalysts.						
Catalysts	Zn loading [wt%]	$S_{BET}$ $[m^2g^{-1}]$	$S_{micro}$ $[m^2g^{-1}]$	$S_{extern}$ $[m^2g^{-1}]$	$V_{pore}$ [cm <sup>3</sup> g <sup>-1</sup> ]	Acid amount [mmol/ g]
S-1 1%Zn/ S-1	- 0.93	432 404	297 291	135 113	0.36 0.33	- 0.227
3%Zn/ S-1	3.09	369	279	90	0.29	0.416
5 %Zn/ S-1	4.66	357	272	85	0.29	0.484
10 %Zn/ S-1	9.3	306	240	66	0.26	0.552

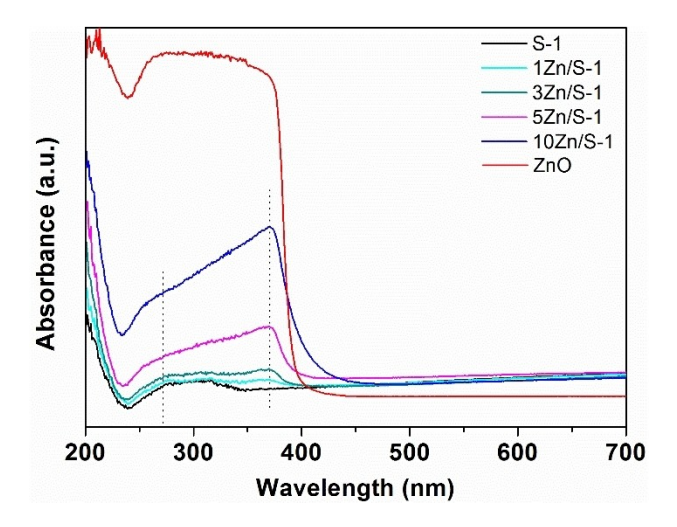
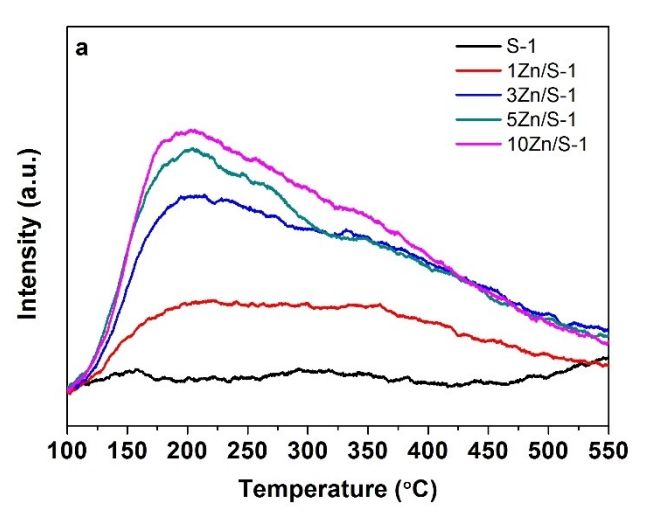


Figure 6. DR UV-vis spectra of the catalysts



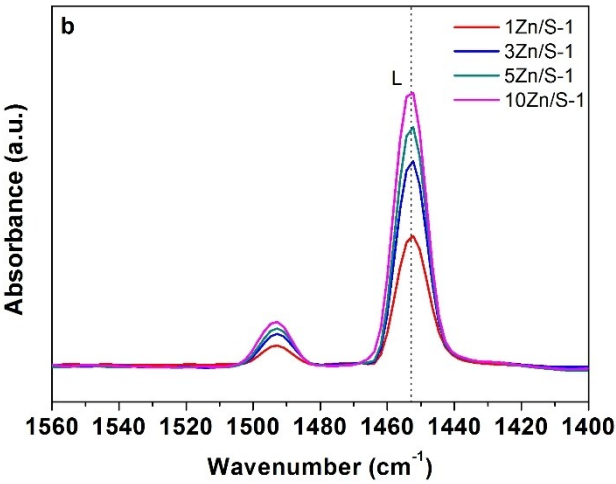


Figure 7. (a) NH<sub>3</sub>-TPD profiles of S-1 and Zn/S-1 catalysts; (b) Py-IR profiles at 150°C of Zn/S-1 catalysts.

has a slight signal of NH3 desorption, demonstrating its weak acidic property. However, the acid amount of catalysts is significantly improved after supporting ZnO with the desorption peaks of Zn/S-1 catalysts falling in similar temperature range from 100-500°C. The Py-IR spectra in Fig. 7b further show that the Zn/S-1 catalysts exhibit Lewis acidity, confirmed by the infrared band at 1453 cm<sup>-1</sup> and no Brønsted acid sites (1540 cm<sup>-1</sup>) are decteted.<sup>[30]</sup> The amounts of Lewis acid sites determined from the NH<sub>3</sub> desorption amounts gradually increase with the increase of Zn loading. Concretely, the acid amount increase from 0.227 mmol/g (1%Zn/S-1) to 0.416 mmol/g (3 %Zn/S-1), 0.484 mmol/g (5 %Zn/S-1) and 0.552 mmol/g (10 %Zn/S-1).

The XPS spectra in Figure 8 shows the spin-orbit splitting value of the Zn 2p peaks in Zn/S-1 is 23 eV, which is typical for Zn<sup>2+[31]</sup> consistent with TEM and UV-vis results. In addition, the binding energy peaks of Zn 2p in Zn/S-1 is 1.1 eV higher than that of ZnO (1045 eV and 1022 eV), suggesting that Zn<sup>2+</sup> becomes more electron deficient.[19] It indicates Si-O-Zn exists considering that the electron density of Zn in the Si-O-Zn bond is lower than that in the Zn-O-Zn bond. The above result

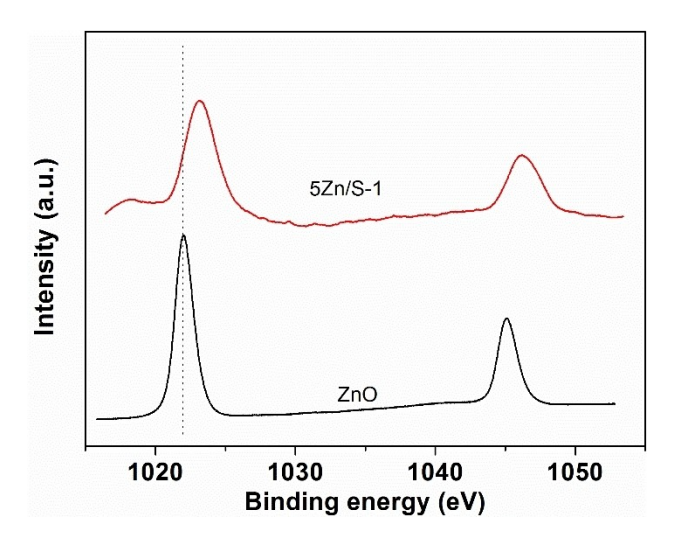
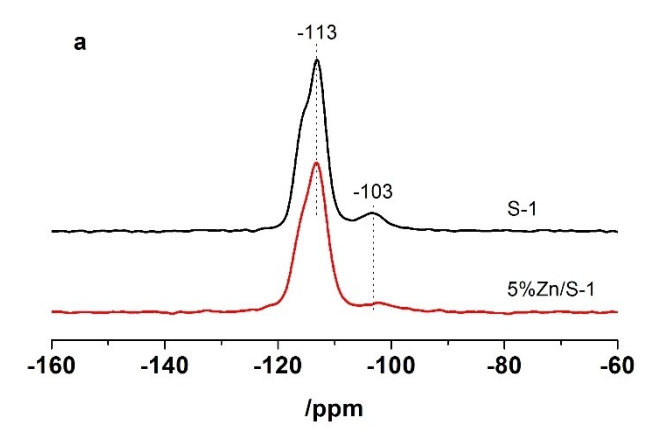


Figure 8. Zn 2p XPS spectra of ZnO and 5%Zn/S-1 catalyst.

indicates interaction develops between the ZnO species and the support. [32]

<sup>29</sup>Si MAS NMR is further applied to explore the interaction between the ZnO species and S-1 zeolite. As shown in Figure 9a, two signals are observed over S-1. The Q<sup>4</sup> signal at -113 ppm is generally assigned to Si(Si-O)<sub>4</sub> while the Q<sup>3</sup> signal at around -103 ppm is attributed to (Si-OH)(Si-O)<sub>3</sub> group.<sup>[33]</sup> After the introduction of Zn, the intensity of the -103 ppm signal significantly declines, indicating the consumption of silanol groups by interaction with ZnO species. FT-IR is applied to characterize the hydroxyl groups on S-1 and Zn/S-1 catalysts. As shown in Figure 9b, there are two major types of -OH groups present for S-1 zeolite. The band at 3731 cm<sup>-1</sup> is attributed to isolated silanol groups exposed on external surface while the broad band centered at 3500 cm<sup>-1</sup> is generally characteristic of silanol nests.<sup>[28,34]</sup> The presence of abundant silanol groups indicates the existence of a large number of defects in S-1 zeolite.[35] After the introduction of Zn species at increasing loading, the peak at 3731 cm<sup>-1</sup> weakens slightly. In comparison, the decreased intensity of the 3500 cm<sup>-1</sup> signal is much more significant, indicating that ZnO species are attached to the support mainly through interaction with the silanol nests. In addition, with the increasing Zn loading to 3%, a new band appears at 3672 cm<sup>-1</sup>, which may arise from the external Zn-OH groups.[36]

Yue et al. reported that silanol groups were important for the dispersion of active chromium and  $GaO_x$  species onto Naform ZSM-5 support in PDH reaction with silanol nests more helpful. Better dispersion of active species can be obtained by interaction between silanol nests and  $CrO_x/GaO_x$  species, resulting in higher dehydrogenation activity thereof. For S-1 supported ZnO catalysts in our work, silanol groups especially silanol nests should have the similar effect. The interaction between silanol nests and ZnO species also suppresses aggregation of ZnO species under reaction conditions, as verified by TEM. Therefore, dispersed active ZnO species through interaction with abundant silanol nests lead to



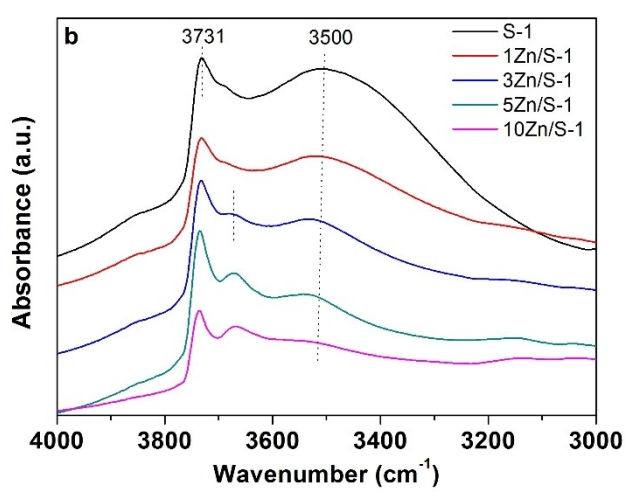


Figure 9. (a)  $^{29}$ Si MAS NMR spectra of selected catalysts; (b) FT-IR spectra of S-1 and Zn/S-1 catalysts.

excellent PDH catalytic performance. Furthermore, TGA shows that the amount of coke over the spent  $5\,\%$ Zn/S-1 catalyst after 6 h reaction at  $550\,^{\circ}$ C and a space velocity  $8000\,\text{mL}\,\text{g}^{-1}\,\text{h}^{-1}$  is determined to be as low as  $2.03\,\%$  (Figure S4). The good anticoking ability is another reason for the reaction stability in PDH.

## Conclusion

In summary, S-1 zeolite has been demonstrated to be a good support for dispersion and stabilization of ZnO species. ZnO species interact with silanol nests of S-1 zeolite. Thus, the resulting Zn/S-1 catalysts exhibit excellent PDH catalytic performance. For instance, propane conversion reaches 49% and propylene selectivity is around 90% under the conditions of 550 °C, 0.1 Mpa and a space velocity 5000 mL h $^{-1}$  g<sub>cat</sub> $^{-1}$ . By contrast, propane conversion is only 0.32% and 1.67% over 5% Zn/SiO<sub>2</sub> and 5%Zn/Al<sub>2</sub>O<sub>3</sub>, and propylene selectivity is 39.8% over 5%Zn/H-ZSM-5. The 5%Zn/S-1 delivers a stable performance within a 6 h PDH test and there is little coke detected.



# **Experimental Section**

#### **Catalyst preparation**

S-1 zeolite was synthesized as follows. 41.66 g tetraethyl orthosilicate (TEOS) and 40.67 g tetrapropylammonium hydroxide (TPAOH, 25 wt%) were mixed to form a clear solution. The obtained solution was stirred for 4 h at room temperature to fully hydrolyze TEOS. Then, it was placed in a 150 mL Teflon stainless-steel autoclave to crystallize at 170 °C for 24 h under static conditions. The precipitate was obtained by centrifugation, washed three times with deionized water, and then dried at 80 °C overnight, which was followed by calcination in air at 550 °C for 4 h.

The S-1 supported ZnO was prepared by impregnation method. The appropriate amount of  $Zn(NO_3)_2 \cdot 6H_2O$  was dissolved in a certain amount of deionized water and then 2 g S-1 zeolite was added to the above solution. The mixture was sonicated and then dried in a rotary evaporator. Then the sample was dried at  $80\,^{\circ}\text{C}$  overnight and calcined at  $550\,^{\circ}\text{C}$  for 4 h in air to obtain n%Zn/S-1 (nZn/S-1) catalyst where n% (n) represented the weight percentage of Zn. For comparison,  $5\,^{\circ}\text{C}$  Zn was also supported on SiO<sub>2</sub> (fumed silica,  $380\,\text{m}^2/\text{g})$ , Al<sub>2</sub>O<sub>3</sub> and H-ZSM-5 (SiO<sub>2</sub>/Al<sub>2</sub>O<sub>3</sub> ratio of 360, purchased from Catalyst plant of Nankai University) following the same procedure and the obtained catalysts were named as  $5\,^{\circ}\text{C}\text{Z}\text{n}/\text{SiO}_2$ ,  $5\,^{\circ}\text{C}\text{n}/\text{Al}_2\text{O}_3$  and  $5\,^{\circ}\text{C}\text{n}/\text{H-ZSM-5}$ , respectively.

#### Catalyst characterization

X-ray diffraction (XRD) patterns of all the catalysts were obtained on a PANalytical X'Pert PRO X-ray diffractometer with Cu  $K\alpha$  radiation.  $N_2$  adsorption and desorption were measured at a Micromeritics ASAP 2020 instrument at 77 K. Before the measurement, the sample was degassed in vacuum at 625 K for 4 h. The Zn loadings were measured on a Philips Magix-601 XRF spectrometer. Transmission electron microscopes (TEM) and Energy dispersive spectroscopy (EDS) were performed on a JEM-2100 and JEM-2100F microscope operating at 200 kV, respectively. Scanning electron microscopes (SEM) images were recorded on a Hitachi SU8020 instrument.

Temperature-programmed desorption of  $NH_3$  ( $NH_3$ -TPD) experiments were conducted on the Micromeritics AutoChem 2920 analyzer. Before the measurement, the sample (100 mg) was firstly treated with He at 550 °C for 1 h. Then, the sample was cooled to 100 °C and 10 %  $NH_3$ /He was introduced into the sample keeping 100 °C for 30 min followed by flushing with He. Subsequently, the sample was heated in flowing He at a rate of 10 °C min $^{-1}$  with desorbed  $NH_3$  recorded using a TCD detector.

Diffuse reflectance UV-vis (DR UV-vis) spectra were recorded on a VARIAN Cary-5000 UV-vis-NIR spectrophotometer with BaSO<sub>4</sub> used as a reference. X-ray photoelectron spectroscopy (XPS) spectra were recorded with an ESCALAB 250Xi spectrometer using monochromatized Al  $\mbox{K}\alpha$  radiation. The binding energy of C1s at 284.8 eV was used as the reference. <sup>29</sup>Si MAS NMR measurements were performed on a Bruker Avance III 600 spectrometer equipped with a 14.1 T wide-bore magnet at a resonance frequency of 119.2 MHz. The spectra were recorded with a high power proton decoupling sequence at a spinning rate of 8 KHz. Chemical shift of <sup>29</sup>Si spectra was referenced to kaolinite at -91.5 ppm. Fourier transform infrared (FT-IR) spectra were measured at 150°C on a Bruker tensor 27 instrument with the samples pretreated at 450 °C in N<sub>2</sub> flow for 1 h. Pyridine adsorption experiment (Py-IR) was carried out on a Bruker XF808-04 Spectrometer. The sample was pressed into a thin self-supporting wafer and pretreated in a vacuum at 500 °C for 30 min. Then the sample adsorbed pyridine

for 5 min after cooling to  $30\,^{\circ}\text{C}$  and the physically adsorbed pyridine was removed in a vacuum at  $150\,^{\circ}\text{C}$  for 30 min.

Thermogravimetric analysis (TGA) was performed on a TA SDT Q600 instrument with the heating rate of 10 °C min<sup>-1</sup> from room temperature to 900 °C in a flowing air.

#### Catalytic activity measurement

PDH reaction was carried out in a fixed-bed stainless steel reactor. In a typical test, 0.3 g catalyst (40–60 mesh) diluted with 0.5 g SiO<sub>2</sub> (40–60 mesh) was loaded in the reactor and heated to 400 °C for 1 h and 550 °C for 1 h in N<sub>2</sub> flow (30 mL min $^{-1}$ ). The feed gas (5% C<sub>3</sub>H<sub>8</sub>, balanced by Ar) was fed into the reactor at 25 mL min $^{-1}$  and atmospheric pressure. The effluents were analyzed by an on-line gas chromatograph (Agilent 7890B) equipped with a flame ionization detector (FID) and a thermal conductivity detector (TCD). The sampling was started 5 min after the feeding of reactant gas. Propane conversion (X<sub>C3H8</sub>) and propylene selectivity (S<sub>C3H6</sub>) were calculated on a carbon atom basis according to the following equations with moles of carbon determined according to the peak area of effluents measured by FID. The selectivity of other products is calculated as the same method as the selectivity to propylene

 $X_{\text{C3H8}} = \frac{\text{moles of total carbon - moles of carbon in propane}}{\text{moles of total carbon}} *100\%$   $S_{\text{C3H6}} = \frac{\text{moles of carbon in propylene}}{\text{moles of total carbon - moles of carbon in propane}} *100\%$ 

# **Acknowledgements**

This work was supported by the National Natural Science Foundation of China (21972141), and the "Transformational Technologies for Clean Energy and Demonstration", Strategic Priority Research Program of the Chinese Academy of Sciences (XDA21030100).

#### **Conflict of Interest**

There are no conflicts to declare.

**Keywords:** Propane dehydrogenation  $\cdot$  Silicalite-1  $\cdot$  Silanol nests  $\cdot$  ZnO species

- [1] S. Chen, X. Chang, G. Sun, T. Zhang, Y. Xu, Y. Wang, C. Pei, J. Gong, Chem. Soc. Rev. 2021, 50, 3315–3354.
- [2] L. Li, W. Zhu, Y. Liu, L. Shi, H. Liu, Y. Ni, S. Liu, H. Zhou, Z. Liu, RSC Adv. 2015, 5, 56304–56310.
- [3] J. Sattler, J. Ruiz-Martinez, E. Santillan-Jimenez, B. M. Weckhuysen, Chem. Rev. 2014, 114, 10613–10653.
- [4] L. Li, W. Zhu, L. Shi, Y. Liu, H. Liu, Y. Ni, S. Liu, H. Zhou, Z. Liu, Chin. J. Catal. 2016, 37, 359–366.
- [5] Z. P. Hu, D. Yang, Z. Wang, Z. Y. Yuan, Chin. J. Catal. 2019, 40, 1233– 1254.
- [6] O. A. Barias, A. Holmen, E. A. Blekkan, J. Catal. 1996, 158, 1-12.
- H. Xiong, S. Lin, J. Goetze, P. Pletcher, H. Guo, L. Kovarik, K. Artyushkova,
   B. M. Weckhuysen, A. K. Datye, Angew. Chem. Int. Ed. 2017, 56, 8986–8991; Angew. Chem. 2017, 129, 9114–9119.



© 2021 Wiley-VCH GmbH

- [8] L. Rochlitz, K. Searles, J. Alfke, D. Zemlyanov, O. V. Safonova, C. Coperet, Chem. Sci. 2020, 11, 1549–1555.
- [9] Z.-P. Hu, Z. Wang, Z.-Y. Yuan, J. Mol. Catal. 2020, 493, 111052.
- [10] V. Z. Fridman, R. Xing, Appl. Catal. A 2017, 530, 154–165.
- [11] S. M. T. Almutairi, B. Mezari, P. C. M. M. Magusin, E. A. Pidko, E. J. M. Hensen, ACS Catal. 2011, 2, 71–83.
- [12] G. Liu, Z.-J. Zhao, T. Wu, L. Zeng, J. Gong, ACS Catal. 2016, 6, 5207–5214.
- [13] T. Otroshchenko, S. Sokolov, M. Stoyanova, V. A. Kondratenko, U. Rodemerck, D. Linke, E. V. Kondratenko, Angew. Chem. Int. Ed. 2015, 54, 15880–15883; Angew. Chem. 2015, 127, 16107–16111.
- [14] B. Hu, W-G. Kim, T. P. Sulmonetti, M. L. Sarazen, S. Tan, J. So, Y. Liu, R. S. Dixit, S. Nair, C. W. Jones, ChemCatChem 2017, 9, 3330–3337.
- [15] B. Hu, N. M. Schweitzer, G. Zhang, S. J. Kraft, D. J. Childers, M. P. Lanci, J. T. Miller, A. S. Hock, ACS Catal. 2015, 5, 3494–3503.
- [16] Y. Dai, X. Gao, Q. Wang, X. Wan, C. Zhou, Y. Yang, Chem. Soc. Rev. 2021, 50, 5590–5630.
- [17] C. Chen, Z. Hu, J. Ren, S. Zhang, Z. Wang, Z.-Y. Yuan, ChemCatChem 2019, 11, 868–877.
- [18] N. M. Schweitzer, B. Hu, U. Das, H. Kim, J. Greeley, L. A. Curtiss, P. C. Stair, J. T. Miller, A. S. Hock, ACS Catal. 2014, 4, 1091–1098.
- [19] S. Han, D. Zhao, T. Otroshchenko, H. Lund, U. Bentrup, V. A. Kondratenko, N. Rockstroh, S. Bartling, D. E. Doronkin, J.-D. Grunwaldt, U. Rodemerck, D. Linke, M. Gao, G. Jiang, E. V. Kondratenko, ACS Catal. 2020, 10, 8933–8949.
- [20] G. Liu, L. Zeng, Z.-J. Zhao, H. Tian, T. Wu, J. Gong, ACS Catal. 2016, 6, 2158–2162.
- [21] C. Chen, Z.-P. Hu, J.-T. Ren, S. Zhang, Z. Wang, Z.-Y. Yuan, J. Mol. Catal. 2019, 476, 110508.
- [22] L. Xie, R. Wang, Y. Chai, X. Weng, N. Guan, L. Li, J. Energy Chem. 2021.
- [23] Y. Cheng, T. Lei, C. Miao, W. Hua, Y. Yue, Z. Gao, Catal. Lett. 2018, 148, 1375–1382.
- [24] G. Liu, J. Liu, N. He, C. Miao, J. Wang, Q. Xin, H. Guo, RSC Adv. 2018, 8, 18663–18671.

- [25] L. Benco, T. Bucko, J. Hafner, J. Catal. 2011, 277, 104–116.
- [26] Y. Cheng, T. Lei, C. Miao, W. Hua, Y. Yue, Z. Gao, Microporous Mesoporous Mater. 2018, 268, 235–242.
- [27] W. Zhou, J. Liu, J. Wang, L. Lin, N. He, X. Zhang, H. Guo, Catalysts 2019, 9, 571.
- [28] Y. Luo, C. Miao, Y. Yue, W. Hua, Z. Gao, Microporous Mesoporous Mater. 2020, 294, 109864.
- [29] J. Chen, Z. Feng, P. Ying, C. Li, J. Phys. Chem. B 2004, 108, 12669-12676.
- [30] Z. Wang, H. Wang, C. Yang, S. Wang, P. Gao, Y. Sun, Ind. Eng. Chem. Res. 2021, 60, 5783–5791.
- [31] J. Zhao, C. Xie, L. Yang, S. Zhang, G. Zhang, Z. Cai, Appl. Surf. Sci. 2015, 330, 126–133.
- [32] Q. Jiang, Z. Wu, Y. Wang, Y. Cao, C. Zhou, J. Zhu, J. Mater. Chem. 2006, 16, 1536–1542.
- [33] C. Ge, X. Sun, D. Lian, Z. Li, J. Wu, Catal. Lett. 2020, 151, 1488–1498.
- [34] J. Zhang, X. Zhu, G. Wang, P. Wang, Z. Meng, C. Li, Chem. Eng. J. 2017, 327, 278–285.
- [35] I. Grosskreuz, H. Gies, B. Marler, Microporous Mesoporous Mater. 2020, 291, 109683.
- [36] Y. Kolyagin, V. Ordomsky, Y. Khimyak, A. Rebrov, F. Fajula, I. Ivanova, J. Catal. 2006, 238, 122–133.
- [37] Y. Cheng, C. Miao, W. Hua, Y. Yue, Z. Gao, Appl. Catal. A 2017, 532, 111– 119.

Manuscript received: July 15, 2021
Revised manuscript received: August 10, 2021
Accepted manuscript online: August 11, 2021
Version of record online:

# **FULL PAPERS**

Silicalite-1 supported ZnO catalysts were prepared by a simple impregnation method. The as-prepared catalysts exhibited an excellent catalytic activity and stability for PDH reaction. Dispersed ZnO species could be obtained and stabilized via interaction between silanol nests of silicalite-1 support and ZnO species. The interaction between silanol nests and ZnO species could suppress aggregation of ZnO species under reaction conditions.



J. Liu, Prof. Y. Liu\*, Prof. H. Liu, Y. Fu, Dr. Z. Chen, Prof. W. Zhu\*

1 – 8

Silicalite-1 Supported ZnO as an Efficient Catalyst for Direct Propane Dehydrogenation

